Analysis of Dual Band-Reject Filter Unit Cell Based on Miller Loading Effect using Strongly Coupled Parallel Lines

Salman Raju Talluri

Department of Electronics and Communications Engineering, Jaypee University of Information Technology, Solan, Himachal Pradesh, India
Email: salmanraju.talluri@juitsolan.in

Abstract. This paper presents the analysis of a novel unit cell of a dual-band reject filter. This unit cell is proposed by using the Miller loading effect on the band-pass filter. The bandpass filter used in this model is designed from parallel coupled lines. Miller loading effect is used in electronics to change the equivalent impedance at input and output ports by connecting an impedance between the input and output ports. This change in the equivalent impedance at input and output alters the resonant frequencies of the band-pass filter and makes it a dual band-reject filter depending on the nature of impedance that has been connected between the ports. Theoretical and numerical simulations is carried out on circuit models with normalized impedances and normalized resonant frequencies. To validate theoretical and numerical simulations, a microstrip bandpass filter based on parallel coupled lines has been converted into a dual band-reject filter. Full-wave electromagnetic simulations are performed and these simulation results are in good agreement with the theoretical and numerical simulations.

Keywords: Band-pass filters, Band-reject filter, Parallel coupled lines, scattering parameters, Transmission line theory

1. Introduction

With the advancement in technology and the need for efficient utilization of spectrum, multiband systems attracted the interest of the researcher in the communication system area [1]. To eliminate the undesired/spurious responses, the communication system needs a band-reject filter. To suppress the strong interference and improve the system's performance, high-quality low-loss filters are needed.

The band-reject filters are used to suppress the unwanted or spurious responses in communication systems. There were few designs available on the design of single bandpass and band-reject reject filters [2-7]. Conventionally, a band-reject filter was designed with the help of source transformations from the lowpass filter design [8]. Even though there is a standard procedure to design a single band-reject filter with the help of source transformation, there is no standard procedure to design a dual-band reject filter. There are different methods in the literature to design the dual band-reject filters.

However, they are primarily based on the specific application. This paper presents a simple and novel technique to design the dual-band reject filter by introducing the unit cell of the dual band-reject filter. The proposed dual-band reject filter unit cell can be used in cascaded sections to design higher-order filters as a replacement for low-quality factor filters.

2. Problem formulation: principle and methodology

This paper uses the principle of Miller loading [9] to change the equivalent impedance at the input and output ports of a bandpass filter. Along with the Miller principle, the periodicity of the distributed transmission line model has been used. According to transmission line theory, the distributed transmission line model is periodic with a periodicity of half

the wavelength (λ /2). The electrical length is defined as $\theta = \beta L$ where β is the phase constant and L is the length of the line expressed in wavelengths (λ). β is given by $2 \pi / \lambda$. Half-wavelength periodicity (λ /2) implies that the distributed model is periodic with an electrical length (angle) of π radians.

A stand-alone high impedance line of quarter wavelength λ /4 as shown in Figure1 is connected between the input and output ports and its characteristics in terms of scattering parameters (insertion loss S_{21} and return loss S_{11}) are observed as a function of frequency with different magnitudes of impedance. The analytical analysis based on periodicity shows two different reactive impedance behaviors over the entire range. The distinction is being the normalized center frequency π /2. This is to say that for the normalized frequency range from 0 to π /2, its behavior is like an inductive reactance, and from π /2 to π, its behavior is like a capacitive reactance.

The distributed transmission line model is represented as a lumped element network of the lowpass filter in nature with inductors in series branches and capacitors in shunt branches. In general, an L-section or a T-section (or sometimes Pi-section) is used to analyze the transmission line model in distributed elements. If a three-element T-section lumped element lowpass filter model is loaded with a high impedance line (which acts as an inductor from 0 to π radians as mentioned above), due to the Miller loading effect the equivalent input and output impedances are bound to change.
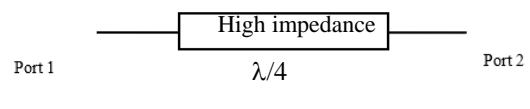
Fig.1 High impedance line between input and output ports.

This change in the impedance at input and output ports can introduce/eliminate poles/zeros and hence this loading can change the nature of the original T-section model. If an inductor is connected, the loaded model can still be a lowpass filter. If a capacitor is connected, the loaded model can becomea band-reject filter.

In the similar manner, a low-pass third-order T-section or Pi-section filter as shown in Figure 2 can be converted into a band-reject filter by connecting the input and output ports with a capacitor. This lowpass to band-reject is primarily because of opposite reactance present in the series branch of T-section or Pi-section model with that connected in Miller loading between input and output port.

Using the duality principle, a third-order high-pass filter is designed by a simple T-section or Pi-section in which the series element is a capacitor and the shunt element is an inductor. This can be converted into a single band-reject filter by connecting the input port and output ports of this T or Pi section filter with an inductor. In both cases, i.e., Miller loading of a lowpass filter and Miller loading of highpass, the band of rejection will depend on the magnitude of the inductor/capacitor that has been connected and the cut-off frequency of the original T or Pi section filter properties.

A band-pass filter has the nature of a high-pass property around the lower cut-off frequency (transition from stop-band to passband). Similarly, the nature of low-pass property around the higher cut-off frequency (transition from passband to stopband). To make this band-pass filter a dual-band reject filter, the high-pass filter behavior must be connected with an inductor as shown in Figure 3 and for the same band-pass filter, the low-pass behavior must be connected with a capacitor as shown in Figure 4. Since a high impedance line connected between input and output ports is behaving like a series inductor and series capacitor over the entire band of periodicity equally, this high impedance line can convert the bandpass filter to a dual band-reject filter.
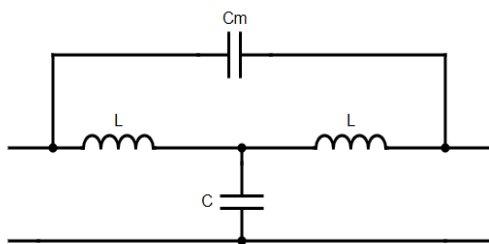
Fig.2 Unit cell of distributed transmission line model loaded with Capacitor in Miller form.
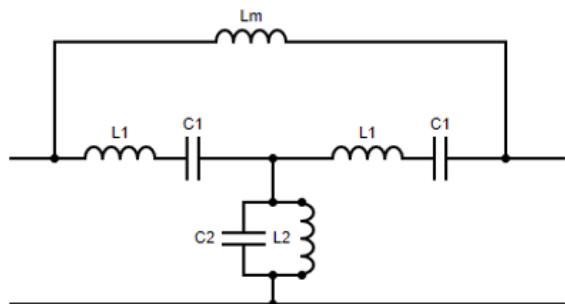
Fig.3 Unit cell of bandpass filter loaded with an inductor in Miller form
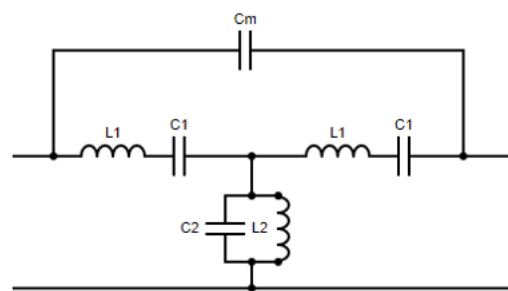
Fig.4 Unit cell of bandpass filter loaded with Capacitor in Miller form

In microwave engineering, band-pass filters are extensively designed using parallel-coupled lines [10]. Hence, the band-pass filter chosen in this paper is designed with the parallel-coupled line theory. In the conventional parallel-coupled line band-pass filters, the coupled line section of length $\lambda/4$ will act as a bandpass resonator. If higher-order filters are needed, cascaded sections of $\lambda/4$ length resonators are used.

A parallel coupled lines structure is characterized by even mode (z_e) and odd mode impedances (z_o). The characteristic impedance of the parallel coupled lines structure (z_c) is generally considered as the average of even mode and odd mode impedances. These even mode impedance and odd mode impedances depend on width (W) and gap (S) between the parallel coupled lines structure.

Two parallel coupled lines form a four-port network as shown in Figure 5. It is represented by impedance parameters in terms of even mode impedance and odd mode impedance.

$$z_{11} = z_{22} = z_{33} = z_{44} = -\frac{j}{2}(z_e + z_o)\cot\theta \quad (1)$$

$$z_{12} = z_{21} = z_{34} = z_{43} = -\frac{j}{2}(z_e - z_o)\cot\theta \quad (2)$$

$$z_{13} = z_{31} = z_{24} = z_{42} = -\frac{j}{2}(z_e - z_o)\csc\theta \quad (3)$$

$$z_{14} = z_{41} = z_{23} = z_{32} = -\frac{j}{2}(z_e + z_o)\csc\theta \quad (4)$$

Here θ is the electrical length of the parallel coupled lines. Using these impedance parameters, the frequency response in terms of scattering parameters is obtained with the help of circuit theory.

3. Numerical Simulations

Numerical simulations have been performed in MATLAB [11]. The scattering parameters are obtained by using the ABCD parameters to S-parameters conversion for all the models/circuits considered in this paper [8]. The characteristic impedance of the input and output ports has been taken as 1 (normalized impedance). Initially, the response of a high impedance line has been obtained for different normalized values such as z_m: 0.5, 2.0, 3.0 and 4.0 and are represented in Figure 6.
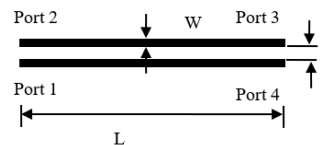
Fig.5 Parallel coupled lines structure
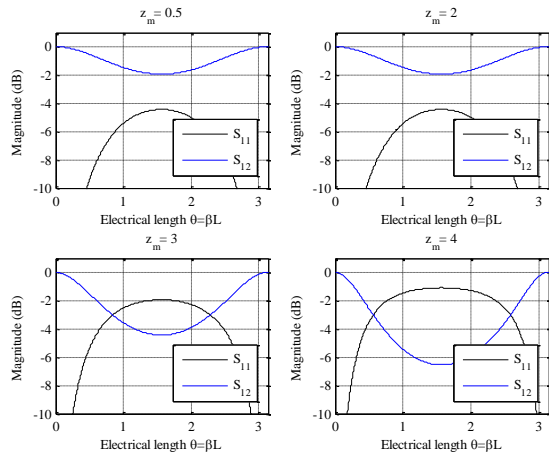
Fig.6 Frequency response of a high impedance line with different characteristic impedance

From this figure, it is observed that the higher the impedance of this line, the variation in transmission and reflection coefficients are more pronounced. From the same figure, it is also observed that the magnitude of S_{21} is decreasing from 0 to $\pi/2$ which is the nature of a series inductor. Moreover, from $\pi/2$ to π, the magnitude of S_{21} is increasing. This is the property of a series capacitor connected between two ports. Hence, the inductive nature from 0 to $\pi/2$ can be used to modify the nature of the high-pass filter to a band-reject filter and the capacitive nature of this transmission line from $\pi/2$ to π can be used to modify the nature of the low-pass filter. By combining both these effects on the band-pass filter, it is possible to design a dual-band reject filter.

The parallel-coupled line model is specified by even mode and odd mode impedances. It has characteristic impedance as the average of even and odd mode impedances. Two sections parallel coupled lines is used in this paper to design a bandpass filter as represented in Figure 7.

The characteristic impedance of the parallel-coupled line has been chosen as 2.5 (fixed normalized impedance) and different responses have been obtained for different even and odd mode impedances to observe the effect of mismatch in the even mode and odd mode impedances. Higher the difference between even and odd mode impedances more is the coupling between the parallel-coupled lines. Fig.8 represents the response for different even and odd mode impedances with fixed characteristic impedance. From this, it is observed that the higher the difference between even and odd mode impedances, the bandwidth is more for the parallel-coupled line.

However, this structure as shown in Fig.8 has to be folded to connect the input and output ports by a high impedance line of length $\lambda/4$ if it is to be converted into a dual band-reject filter.
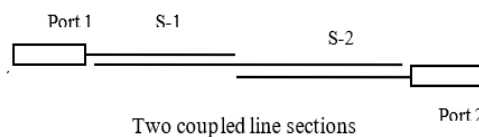
Fig.7 Two sections Parallel coupled lines
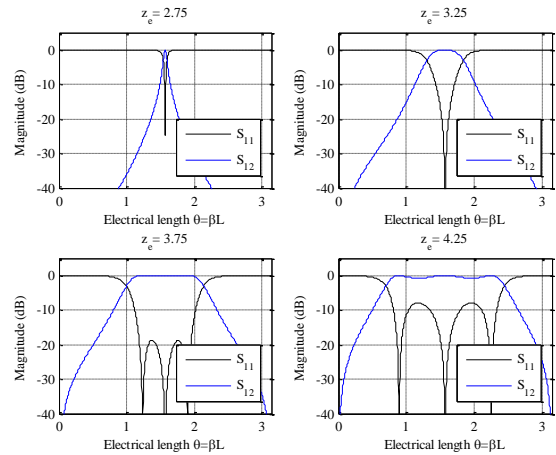
Fig.8 Two section parallel-coupled line bandpass filter response for different even and odd impedances (but with same characteristic impedance) without L x.

A slight modification has been done to this parallel-coupled line filter to provide the flexibility to connect input and output ports by a high impedance line as shown in Figure 9. This folding is done by connecting a connecting line of length L_x between the first section parallel-coupled lines with the second section parallel-coupled line. Here L_x is taken as equal to the coupled line length L_c which is quarter-wavelength. Two different cases have been considered for the numerical simulations to see the effect of this connecting line. From these simulations, it is observed that the $L_x = L_c$ length is providing the needed flat response for the bandpass filter.

Figure 10 represents the frequency response of the PCL bandpass filter with the short connecting line ($L_x = \lambda/8$) in comparison with the coupled line section.
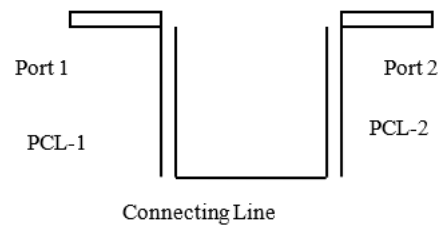
Fig.9 Folded Parallel coupled line section with connecting line
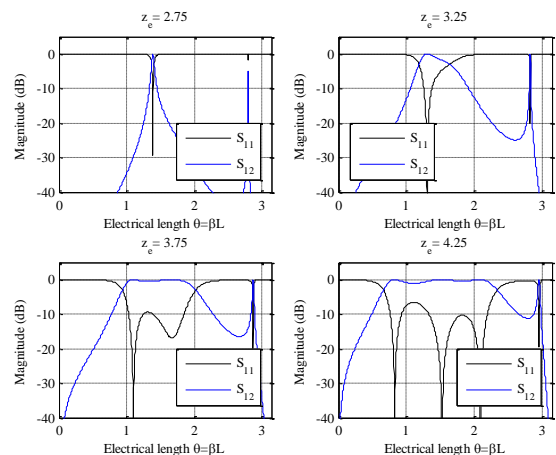
Fig.10 PCL bandpass response with short connecting line.

It is observed that the short length has its dominant effect on the higher frequencies in comparison with the lower frequencies. To preserve the periodicity property the length of this connecting line has been taken as L_c.

Figure 11 represents the response of the response with the connecting length equal to coupled section length. From this figure, it is observed that there is some ripple in the passband. However, there is a widening of the bandpass filter response.

Finally, Figure 12 represents the response of the two-section PCL filter after adding the high impedance line. Even though there is a ripple initially, it has been minimized in the final dual-band reject filter. From this figure, it is observed that the above-mentioned principle of conversion of bandpass into dual band-reject filter has in agreement with the numerical simulations.

4. Full-wave electromagnetic simulations

The above-mentioned procedure in the numerical simulations has been converted into a layout on microstrip substrate of RT duroid (RT5880 $\epsilon_r = 1.1$ with loss tangent of 0.0009). The layouts for circuits considered are represented in figures from Fig.13 to Fig.16. In order to obtain the return loss and insertion loss, transient response has been used in the CST microwave studio.The design specifications for the layouts are mentioned in Table1.

Fig.11 Two section parallel-coupled line bandpass filter response with $L_x = L_c$.

Fig.12 Dual band-reject filter response.
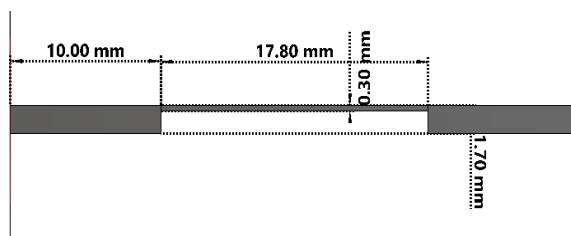
Fig.13 Layout of high impedance line.
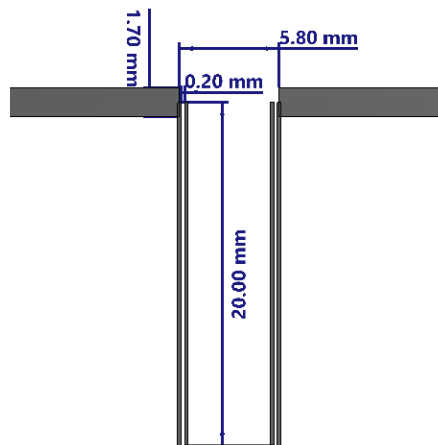
Fig.14 Layout of two sections parallel coupled lines structure with a short connecting line.
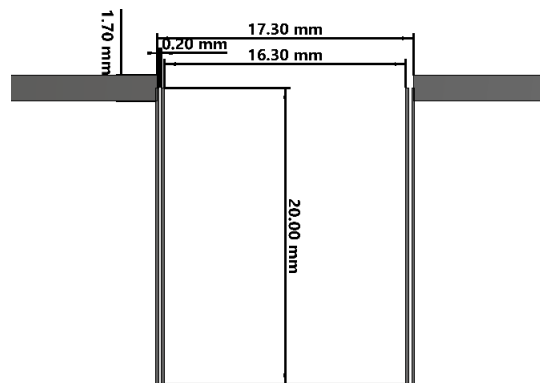
Fig.15 Layout of two sections parallel coupled lines structure with $\lambda/4$ connecting length.
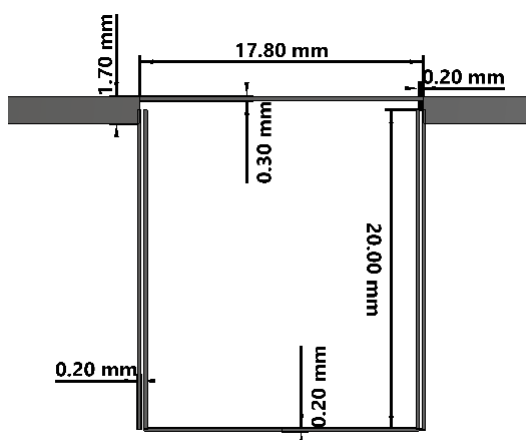
Fig.16 Layout of two sections parallel coupled lines structure with $\lambda/4$ connecting length with Miller loading.
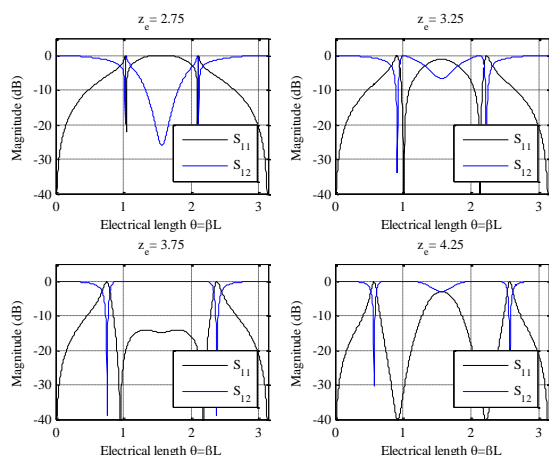
Table 1: The parameters used in the design

S.No	Parameter	Value (in mm)
1	Length of the coupled line	20
2	Separation between the coupled lines	0.2
3	Width of the coupled line	0.2
4	Length of the feed line	10
5	Width of the feed line	1.7
6	Width of the high impedance line	0.3
7	Thickness of the conductor	0.0335
8	Length of the connecting line	8.25
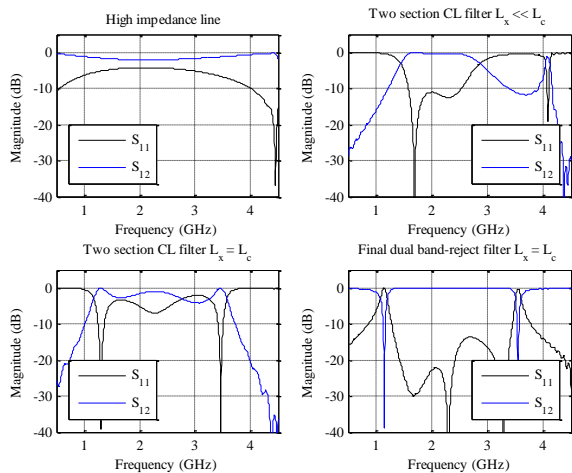
Fig.17 Simulated results of dual band-reject filter response with Miller loading

Fig.17 represents the responses of the circuits from the full-wave simulations. An optimization has been performed on the Miller loaded structure and the optimal response of dual-band reject filter is occurring at a reduced length of 17 mm in comparison with 20 mm. This can be because of the mismatch in the exact dimensions calculations at the feeding line connections at port 1 and port 2. From this figure, it is very clear that the above-mentioned numerical results are in very good agreement with the full-wave simulations validating the design procedure. Further analysis can be pursued to present the design graphs/nomograms to control the bandwidths of the rejection bands and passbands.

5. Conclusion

A simple novel unit cell to design a dual band-reject filter based on Miller loading and periodicity of the distributed transmission line model has been presented. Numerical simulations based on the theoretical concept have been developed and validated by converting the circuits onto microstrip layouts. The bandpass filter is designed using the parallel-coupled line theory and this bandpass filter has been converted into a dual band-reject filter by Miller loading. From the full-wave electromagnetic simulation results, the characteristics of the designed dual-band reject filter is in good agreement with the numerical simulations thereby validating the design procedure.

References

[1] D. Psychogiou, R. Gomez-Garcia, and D. Peroulis, RF wide-band bandpass filter with dynamic in-band multi-interference suppression capability, *IEEE Transactions on Circuits and Systems II: Express Briefs*, vol. 65, no. 7, pp. 898-902, 2018.

[2] H. Wang, K. Tam, W. Choi, W. Zhuang, S. Ho, W. Kang, and W. Wu, Analysis of coupled cross-shaped resonator and its application to differential bandpass filters design, *IEEE Transactions on Microwave Theory and Techniques*, vol. 62, no. 12, pp. 2942-2953, 2014.

[3] S. Kumar, R. D. Gupta, and M. S. Parihar, Multiple band notched filter using c-shaped and e-shaped resonator for uwb applications, *IEEE Microwave and Wireless Components Letters*, vol. 26, no. 5, pp. 340-342, 2016.

[4] L. Zhou, Y. Ma, J. Shi, J. Chen, and W. Che, Differential dual-band bandpass filter with tunable lower band using embedded dgs unit for common-mode suppression, *IEEE Transactions on Microwave Theory and Techniques*, vol. 64, no. 12, pp. 4183-4191, 2016.

[5] F. Bagci, A. Fernández-Prieto, A. Lujambio, J. Martel, J. Bernal, and F. Medina, Compact balanced dual-band bandpass filter based on modified coupled-embedded resonators, *IEEE Microwave and Wireless Components Letters*, vol. 27, no. 1, pp. 31-33, 2017.

[6] Y. Huang, J. Bao, G. Tang, Q. Zhang, T. Omori, and K. Hashimoto, Design consideration of saw/baw band reject filters embedded in impedance converter, *IEEE Transactions on Ultrasonics, Ferroelectrics, and Frequency Control*, vol. 64, no. 9, pp. 1368-1374, 2017.

[7] J. Sorocki, I. Piekarz, S. Gruszczynski, and K. Wincza, Low-loss directional filters based on differential band-reject filters with improved isolation using phase inverter, *IEEE Microwave and Wireless Components Letters*, vol. 28, no. 4, pp. 314-316, 2018.

[8] D. M. Pozar, *Microwave Engineering*. John wiley & sons, 2011.

[9] A. S. Sedra and K. C. Smith, *Microelectronic circuits*. New York: Oxford University Press, 1998, vol. 1.

[10] C. Caloz and T. Itoh, *Electromagnetic metamaterials: transmission line theory and microwave applications*. John Wiley & Sons, 2005.

[11] MATLAB, version 7.10.0 (R2010a). Natick, Massachusetts: The MathWorks Inc., 2010.

[12] CST Microwave, and M. CST. "CST Microwave studio." CST Studio Suite).

Biography of the author

Salman Raju Talluri: He completed his M.Tech from IITK in 2009 and obtained his Ph.D titled "Analysis of non-linear transmission lines for opposite phase and group velocities" in 2017 from Jaypee University of Information Technology with title, Solan, Himachal Pradesh, India. His areas of interest include non-linear transmission lines, microwave engineering and antenna arrays. He is currently working as an assistant professor in Jaypee University of information Technology, Solan. He was with the Astra microwave products limited, Hyderabad for one year 2006 to 2007.